Generation of strength in a drying film: How fracture toughness depends on dispersion properties

Natalie Birk-Braun[1], Kamran Yunus[2], Eric Rees[2], Wilhelm Schabel[1], Alexander Routh[2]*

1. Karlsruhe Institute of Technology, Kaiserstr. 12, 76131 Karlsruhe, Germany
2. Department of Chemical Engineering and Biotechnology, Pembroke Street, Cambridge, CB2 3RA

Abstract

The fracture toughness of colloidal films is measured by characterising cracks which form during directional drying. Images from a confocal microscope are processed to measure the crack width as a function of distance from the crack tip. Applying theory for thin elastic films the fracture toughness is extracted. It is found that the fracture toughness scales with the particle size to the -0.8 power and that the critical energy release rate scales with the particle size to the -1.3 power. In addition, the fracture toughness is found to increase at lower evaporation rates, but the film thickness does not have a significant effect.

Introduction

Particulate coatings are omnipresent in our daily lives, commonly used to modify the properties or visual appearance of surfaces. They are often manufactured by drying a thin continuous layer of colloidal dispersion. A common observation is the appearance of cracks and these have a detrimental effect on the film performance [1].

When the drying process is initiated, the particles first order at the film edge and form a particle network. This results in a front of packed particles propagating across the film, due to continued evaporation of solvent from the consolidated region. The flow of solvent through this consolidated region results in a pressure drop along the packed region [1], which is responsible for the eventual cracking of the film [2].

Within the film the stress intensity factor, *K*, is dependent on sample geometry, sample material, applied load, crack location and crack size. At the instant of crack propagation, the stress intensity factor reaches a critical value, K_c, also known as the fracture toughness. This value defines the materials resistance to fracture [3]. Drying films are transitioning from a liquid to a solid. Consequently, one expects the fracture toughness to increase from a low value in the fluid, to a larger value in the film.

Cracks in thin films of elastic material [4] are well understood. For particulate coatings, it is widely accepted that the driving force for cracking is the capillary pressure, which scales with the inverse of particle size. Consequently, films of smaller particles are expected, and observed, to crack more readily [5]. This argument however ignores the effect of particle size on the material parameters resisting cracking. Goehring et al [3], examined the crack shape and applied expressions for elastic films. This allowed an estimate of the film fracture toughness to be made and no effect of the particle size was observed. Data for other particle materials, film thicknesses or evaporation rates, however, are not yet available. The purpose of this work is, for the first time, to investigate the effect of various dispersion and processing parameters on the film fracture toughness.

A thin elastic film theory [4, 6] was developed for a film in which the crack walls are pulled apart by the influence of a normal tensile stress. The shape of the crack is predicted to follow

$$\delta = \frac{8K_c}{E}\sqrt{\frac{r}{2\pi}} \qquad (1)$$

Where δ is the crack opening and *r* in the distance from the crack tip. The theory predicts that the ratio of critical stress intensity factor over Young's Modulus, K_c/E, can be calculated, by measuring the shape of cracks. Equation 1 applies for linear elastic materials. The other restrictions are that any plastic zone, around the crack tip, must be small and the crack length must be less than the film thickness [3, 4, 7, 8, 9].

To determine the fracture toughness, the elastic modulus has to be estimated. Equation 2 was developed for dry powder compacts [10, 11].

$$E = 7.63 \cdot \phi^4 \left(\frac{E_p^2 \cdot 2 \cdot \gamma_p}{a}\right)^{1/3} \qquad (2)$$

where E_p is the elastic modulus of the particle material, a the particle radius, ϕ the volume fraction of the particle network and γ_p the interfacial energy of the particle material. We adapt this equation to use the surface

tension of the particle material in water and hence determine the modulus for the wet compact. The values used for the moduli and surface energies are shown in Table 1. The value for volume fraction was simply taken as 0.64.

For linear elastic materials, the fracture toughness is defined as the square root of the critical energy release rate, G_c, times the Young's Modulus [4].

$$K_c = \sqrt{G_c \times E} \tag{3}$$

The energy release rate describes the amount of energy released due to the creation of crack surface [17, 18]. Tirumkudulu and Russel argued that G_c is constant and approximated by the surface energy of water [5]. Consequently, one expects the fracture toughness to scale with the particle size as, $K_c \sim a^{-1/6}$. The same scaling prediction was presented by Goehring et al. [3] with the comment that a larger range of particle sizes, than used in their experiments, would be needed to observe such an effect.

Kendall [11], considering dry powder compacts, presents a different scaling, where the critical energy release rate is particle size dependent and follows as

$$G_c = 56\phi^4 \left(\frac{\gamma^5}{E_p^2 a^2} \right)^{1/3} \tag{4}$$

with γ the energy to create surface. This is found to be higher than γ_p because it includes the energy losses associated with fracture creation. Using equations 2, 3, and 4, the scaling for fracture toughness is derived as $K_c \sim a^{-1/2}$. For an experimental investigation, Kendall uses titania and alumina particles mixed with aqueous solutions of polyvinyl alcohol and then heated to burn out the polymers. Using particles of various sizes, he confirms the $a^{-1/2}$ relation as well as the expected dependence on ϕ^4.

In this work we seek to determine the effect of particle size on the fracture toughness of drying thin films. We use two different particle types: silica and polystyrene, and examine six different particle sizes.

Materials and Methods

Our experiments consider colloidal dispersions of silica and polystyrene particles with particle diameters between 7 and 450 nm as well as varying film thicknesses and evaporation rates. Colloidal films were dried on glass cover slips which were positioned in a custom 3D printed drying rig, with air of known humidity blown gently over the top, as sketched in figure 1. The rig enabled the film to be mounted in an inverted confocal microscope (Leica SP5). The microscope settings were size: 8192 × 8192 pixels; pixel width: 47 nm on sample; objective: 40 × 0.6 NA; pinhole aperture: 141.47 µm; laser wavelengths: 514 nm (20 %), 633 nm (70 %).

The directional drying process was achieved with a filtered (0.2 µm) laminar airflow of 1 litre per minute at constant humidity. The resulting cracks originate at the blown-edge of the sample. They formed with a well-defined spacing and cracking front, in good agreement with the observations of Goehring et al. [3]. The cracks were found to propagate in a stick-slip fashion, as has been reported previously [2]. All investigated colloidal dispersions had an initial particle volume fraction of 10 ± 1 % and the investigated crack lengths were always smaller than the film thickness. The evaporation rate was measured to be constant over the entire experiment. Therefore, we concluded that the drying process did not become hindered by a film side mass transfer resistance or formation of a skin.

The influence of the particle diameter was investigated using three different silica dispersions (Ludox® SM, 7 nm; Ludox® HS-40, 12 nm; Ludox® TM-50, 22 nm all obtained from Sigma Alrdich) and three different polystyrene dispersions all obtained from Sigma Aldrich (Latex beads, polystyrene LB1, 100 nm; LB3, 300 nm; LB5, 450 nm). The particle diameters were determined with a FEI Tecnai F20 transmission electron microscope.

For the dependence of the fracture toughness on film thickness five different volumes of dispersion 4, 8, 12, 16 and 20 mm^3 were considered using 7 nm diameter silica and 300 nm diameter polystyrene.

The effect of evaporation rate was investigated by supplying air streams at four distinct humidity levels, controlled by a molecular sieve (rel. humidity of 1.3 %) and three different supersaturated salt solutions

(magnesium chloride, rel. humidity of 32.3 %; sodium chloride, rel. humidity of 69.6 %; potassium chloride, rel. humidity of 77.8 %).

The images were processed using a MATLAB® script which uses brightness thresholding to extract the size and shape of individual cracks. Typical raw image data for cracks from a silica dispersion are given in Figure 2a, and for a polystyrene dispersion in Figure 2b. Cracks produced in the directional drying setup are identifiable as dark vertical features which widen and split into two dark vertical edges with a bright core as the tip propagates. The MATLAB® script uses thresholding to detect pixels significantly darker than the background grey level, combined with a horizontal infilling method to evaluate the crack width including any core. The crack width evaluated in each horizontal row of pixels can then be related to the distance from the crack tip, which is located in the lowest row of pixels where thresholding detects the distinctly dark signal of the crack. Sample data and the analysis script are provided in the accompanying open-data [19].

Results

Figure 3 shows the average crack opening of all measurements of 89 cracks in 7 nm colloidal silica (red line) and 63 cracks in 300 nm polystyrene beads (green line) for an air humidity of 1.3 % at 20 °C and 4 mm^3 of colloidal dispersion. The presented crack trends are representative for all investigated dispersions. Figure 3 illustrates that for silica particles, close to the crack tip, the crack width agrees well with the predictions of Equation 1. The cracks arising from polystyrene dispersions, however, show some deviation. This may indicate that the plastic zone around the crack tip is larger for polystyrene particles. This observation agrees with the findings of Geohring et al [3], who found that only 20 -30 % of the crack opening in charged-stabilized colloidal polystyrene latex was reversible. The more pronounced plastic deformation in polystyrene based colloidal dispersions may also be due to the softer modulus of the polystyrene particles. Consequently, we conclude that the silica dispersions conform with the elastic theory and the polystyrene dispersions display significant deviations. Nevertheless, both colloidal dispersions were approximated as elastic materials for the evaluation of fracture toughness.

We compute a straight line which provides a best fit for the data presented in Figure 3, yielding, with Equation 1, an estimate of the fracture toughness over Young's Modulus. It was found that for silica based dispersions, the slope of the best fit line varies only marginally when computed for different lengths. For polystyrene based dispersions, however, the slope of the line decreases significantly when computed over longer crack lengths. Furthermore, as shown in Figure 3, the average crack opening for polystyrene dispersions displays more noise compared to the silica dispersions. The result is that the error bar for the polystyrene dispersions is considerably higher than with the silica particles.

Figure 4 shows the dependence of K_c/E on film thickness, evaporation rate and particle size. It can be seen that the volume of colloidal dispersion, i.e. the film thickness, has no influence whereas for increasing humidity, i.e. decreasing evaporation rates, the ratio K_c/E increases.

Figure 4 c and d show the effect of particle size on K_c/E. Generally, the value of K_c/E decreases as the particle size increases. The data point for particles with a diameter of 450 nm, should be taken with caution as the recorded images where opaque and the crack images became blurred. The values for K_c/E determined for the bigger polystyrene particles were found to be larger than for the investigated smaller silica particles. It is not possible to determine if this increase has its origin in the inherent material properties or whether it is an effect of the larger particle size. The value of K_c/E for polystyrene based dispersions of approximately $0.11\sqrt{\mu m}$, reported here, agrees with the measurements by Goehring et al [3]. However, Goehring et al. did not observe a strong particle size dependence on K_c/E for particle diameters between 50 and 100 nm.

Figure 5a shows the dependence of fracture toughness on particle size combining the data for all investigated particle diameters. One observes a decrease in fracture toughness for larger particle sizes. If we assume that the particle material type does not affect the fracture toughness, then we may place a line through all the data points as shown in figure 5a. The slope through the experimental data is -0.8 ± 0.2. This varies from the scaling predictions of a slope of -1/6 and -1/2 which are plotted on Figure 5a. Using this experimentally determined scaling for fracture toughness the critical energy release rate is predicted to scale with the particle size as $G_c \sim a^{-1.3\pm0.4}$.

The graph in Figure 5b shows a slight increase in fracture toughness for both materials as the humidity is increased. This is likely to be due to more ordered particles at slower evaporation rates. An increase in volume fraction will intuitively make a tougher material with more particle-particle bonds needing to be broken.

Discussion

The experimentally found scaling for the dependence of fracture toughness on particle size is $K_c \sim a^{-0.8}$. This is different from the two theoretical scaling predictions but far closer to the prediction of -1/2 from Kendall. The results can be interpreted as the critical energy release rate being dependent on the particle size. This means that breaking the network of particles is contributing to the energy of crack formation. This is contrary to a scaling argument by Tirumkudulu and Russel [5], who suggested that the water-air surface tension was the dominant energy of crack formation. The scaling of fracture toughness with particle size to a power of magnitude less than unity agrees with the common observation that dispersions of smaller particles crack more easily. The capillary pressure scales as a^{-1} and consequently, as the particle size is reduced, the film stress will always increase more quickly than the toughness.

The major assumption of this work is that the modulus and fracture toughness do not change spatially in the film: The derivation of equation 1, assumes a linear elastic material with constant elastic properties. According to Kendall [11], the modulus and fracture toughness are predicted to depend on the particle volume fraction to the fourth power. Hence to assume constant elastic properties necessitates assuming that the particle volume fraction and structure do not change across the compacting region of the film. We have not measured the volume fraction and simply assumed a constant value of 64%. There are experimental measurements of the volume fraction in drying films from Boulogne *et al*. [23], who used SAXS and SANS on various regions of a directionally drying film to demonstrate a flow dependent anisotropy. Crucially, they observed a packing of the particles into a structure with volume fraction of around 64 % irrespective of the numerous conditions they examined. The volume fraction increased further into the compacted region, as the capillary stress increased, but the increase was at best shallow. This is evidence for a weakly spatially varying volume fraction. This will result in a spatially varying modulus and toughness. This provides an explanation for the deviation of Figure 3 from a straight line. If the film becomes tougher and stronger in the compacting region, then a deviation in slope would be expected. To quantify this is difficult since it depends on the local packing and consequently the approach followed here of calculating an *average* fracture toughness for the film seems reasonable. It is also worth noting that the experimental variation in fracture toughness and modulus of the film, as evidenced by the error bars on figures 4 and 5 are not excessive, allowing the statement concerning the particle size dependence on fracture toughness to be made.

The finding that the film thickness does not affect the measured fracture toughness is reassuring, since the fracture toughness is a material property and independent of the sample geometry.

The other finding of this work is that slow evaporation, increases the toughness. This is a well-known observation [20-22] although the present work is, to our knowledge, the first to quantify the effect in terms of fracture toughness. The explanation of increased packing fraction is speculation, although it is difficult to think of any other reasonable reason for the effect of humidity. The particle volume fraction is predicted to have a strong effect with a ϕ^4 scaling for both the modulus and energy release rate. Consequently, only a small increase in volume fraction will have a large effect on the fracture toughness.

Self-ordering of colloidal particles upon drying is controlled by a particle Peclet number. This compares the time necessary for particles to diffuse their own radius to the time available for packing. One estimate of the diffusional time is a^2/D, which assuming a Stokes Einstein diffusion coefficient for D becomes, $6\pi\mu a^3/kT$, with μ the solvent viscosity. The time available for evaporation is H/E with E the evaporation rate and H the film thickness. Consequently, the particle Peclet number is estimated as $6\pi\mu Ea^3/HkT$. For an evaporation rate of 0.3 cm per day [1] from aqueous based films of 100 μm thickness, the particle Peclet number is estimated to be 5 x 10^{-10} for 7 nm particles and 1.5 x 10^{-4} for 450 nm particles. In both cases we estimate that the diffusional time is much smaller than the evaporation time and hence ordering is possible.

There are a couple of caveats to the scaling argument presented above. The Stokes-Einstein diffusion coefficient corresponds to dilute dispersions and here we apply it to a concentrated array of particles. In addition, the time available for diffusion is smaller than our estimate of H/E. This is because the drying front propagates horizontally across the film and it is only the time that the particles are in the presence of the drying front that allows particle rearrangement. We have however previously estimated this time scale to be about 30 times

shorter than the evaporation time [24]: The particle Peclet number is still much less than unity in all cases. This suggests that we will not see a dramatic difference in packing between experiments and so the effect of particle size on fracture toughness is not likely to be due to the change in particle Peclet number causing additional ordering. It also explains why the effect of evaporation on the fracture toughness is only small, as shown in Figure 5b. The change in volume fraction need only be minimal to achieve the observed change in fracture toughness.

Conclusions

We have shown that the fracture toughness of colloidal dispersions can be measured during a directional drying process based on the length and width of observed cracks. The film fracture toughness was measured as a function of colloidal material, particle size, film-thickness and evaporation rate. Our results show that particle size and evaporation rate have a significant influence on fracture toughness.

Acknowledgements

We thank Professor Bill Clegg for helpful discussions, Martin Lippert for help with Matlab as well as the Ernest-Solvay-Stiftung and Studienstiftung des deutschen Volkes for financial support of the research visit of N. Birk-Braun from Karlsruhe Institute of Technology (KIT) to the University of Cambridge.

References

[1] Routh, A. F. *Drying of Thin Colloidal Films*, Reports on Progress in Physics 76 046603 2013.

[2] Dufresne, E. R.; Corwin, E. I.; Greenblatt, N. A.; Ashmore, J.; Wang, D. Y.; Dinsmore, A. D. et al. *Flow and fracture in drying nanoparticle suspensions.* Physical Review Letters 91 (22): 224501 2003.

[3] Goehring, L.; Clegg, W. J.; Routh, A. F. *Plasticity and fracture in drying colloidal films.* Physical Review Letters 110 (2): 024301 2013.

[4] Lawn, B. R. Fracture of brittle solids. 2nd ed. Cambridge, New York: Cambridge University Press 1993.

[5] Tirumkudulu, M. S. and Russel, W. B. *Cracking in Drying Latex Films*, Langmuir 2: 4938-4948 2005.

[6] Hutchinson, J. W.; Suo, Z. *Mixed Mode Cracking in Layered Materials*. Advances in Applied Mechanics (29): 63–191 1992.

[7] Beuth, J. L. *Cracking of thin bonded films in residual tension.* International Journal of Solids and Structures 29 (13): 1657–1675 1992.

[8] Xia, Z. C.; Hutchinson, J. W. *Crack patterns in thin films.* Journal of the Mechanics and Physics of Solids 48 (6-7) 1107–1131 2000.

[9] Xu, Y.; Engl, W. C.; Jerison, E. R.; Wallenstein, K. J.; Hyland, C.; Wilen, L. A.; Dufresne, E. R. *Imaging in-plane and normal stresses near an interface crack using traction force microscopy.* Proceedings of the National Academy of Sciences of the United States of America 107(34):14964-14967 2010.

[10] Thornton, C. *On the relationship between the modulus of particulate media and the surface energy of the constituent particles.* Journal of Physics D: Applied Physics 26 (10): 1587–1591 1993.

[11] Kendall, K. *Agglomerate Strength*. *Powder Metallugry 31 (1): 28–31 1988.*

[12] Kim, M. T. *Influence of substrates on the elastic reaction of films for the microindentation tests*. Thin Solid Films 283 (1-2): 12–16 1996.

[13] Verein Deutscher Ingenieure VDI- Wärmeatlas. [Berechnungsunterlagen für Druckverlust, Wärme- und Stoffübertragung]. 10., bearb. und erw. Aufl. Berlin, Heidelberg [u.a.]: Springer 2006

[14] Rimai, D. S.; Quesnel, D. J.; Busnaina, A. A. *The adhesion of dry particles in the nanometer to micrometer-size range.* Colloids and Surfaces A: Physicochemical and Engineering Aspects 165 (1-3): 3–10 2000.

[15] Okubo, T. *Surface Tension of Structured Colloidal Suspensions of Polystyrene and Silica Spheres at the Air-Water Interface.* Journal of colloid and interface science 171 (1): 55–62 1995.

[16] Russel, W B.; Saville, D. A.; Schowalter, W. R. *Colloidal dispersions*. Cambridge, New York: Cambridge University Press 1989.

[17] Goehring, L.; Clegg, W. J.; Routh, A. F. *Wavy cracks in drying colloidal films*. Soft Matter 7 (18): 7984 2011.

[18] Gauthier, G.; Lazarus, V.; Pauchard, L. *Alternating crack propagation during directional drying. Langmuir 23 (9): 4715–4718 2007.*

[19] Opendata. (2016) Image files and sample matlab scripts to generate crack openings can be found at http://dx.doi.org/10.17863/CAM.885

[20] Mizuno, T.; Nagata, H. and Manabe, S. *Attempts to avoid cracks during drying*, Journal of Non-Crystalline Solids 100: 236-240 1988.

[21] Bou Zeid, W.; Vicente, J. and Brutin, D. *Influence of evaporation rate on cracks' formation of a drying drop of whole blood*, Colloids and Surfaces A 432: 139-146 2013.

[22] Boulogne, F.; Giorgiutti-Dauphine, F. and Pauchard, L. *How to reduce the crack density in drying colloidal material*, Oil & Gas Science and Technology 69(3): 397-404 2014.

[23] Boulogne, F.; Pauchard, L.; Giorgiutti-Dauphine, F.; Botet, R.; Schweins, R.; Sztucki, M.; Li, J.; Cabane, B. and Goehring, L. *Structural anisotropy of directionally dried colloids*, EPL 105: 38005 2014.

[24] Routh, A. F. and Russel, W. B. *Horizontal drying fronts during solvent evaporation from latex films*, AIChE J 44 (9) 2088 1998.

Table 1: Values for material modulus and surface energy in water as well as source references. Note: These are literature values and not specific to the samples used in this work. The modulus values will be pretty accurate whilst the surface energies will depend on any surface groups.

	E_p (N m^{-2})	γ_p (J m^{-2})
Polystyrene	3.3×10^9 [12]	0.0075 [14,15,16]
Silica	67×10^9 [13]	0.0093 [14,15,16]

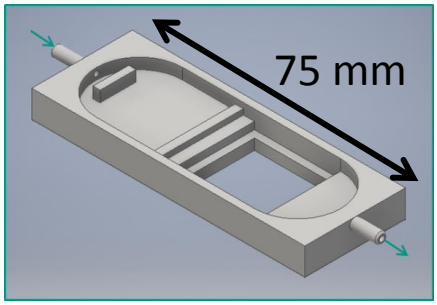

Figure 1: Picture of 3D printed drying chamber. The entire device is 75 mm long, so that it fits within the confocal microscope. There are connections at either end to allow air of known humidity to be blown over the sample.

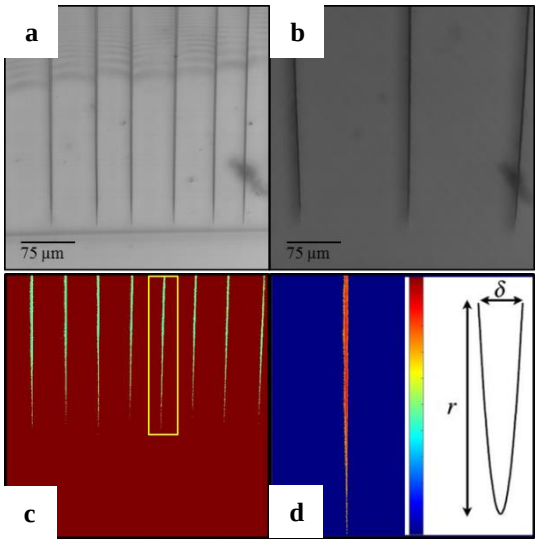

Figure 2: (a) and (b) show the fracture formation in colloidal dispersions containing silica particles and polystyrene particles recorded with a confocal microscope at 20 °C for an air humidity of 1.3 % and a volume of colloidal dispersion of 4 mm^3. (c) shows the image of the colloidal dispersion based on silica particles processed with a MATLAB® script. (d) presents one single crack of picture (c) used for measurements of the crack opening, δ, and the distance, *r*, from the crack tip. The crack geometry is the same as defined by Goehring et al. [3].

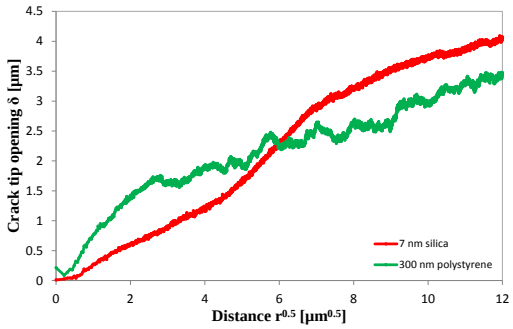

Figure 3: Average crack opening as a function of square root of distance from crack tip for 7 nm colloidal silica (red) and 300 nm polystyrene beads (green) for an air humidity of 1.3 % at 20 °C and a volume of colloidal dispersion of 4 mm^3.

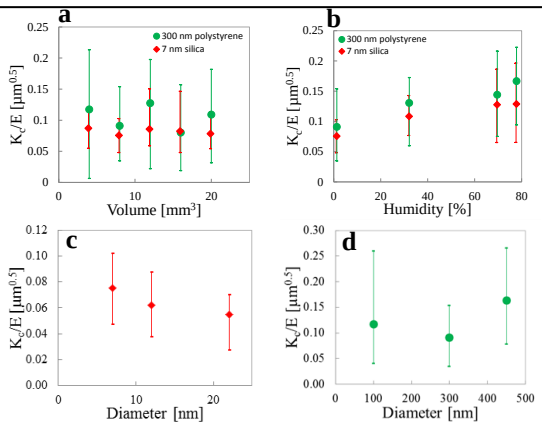

Figure 4: Measured influence on the ratio of fracture toughness over Young's modulus, K_c/E, of colloidal dispersions containing silica particles (red diamond) and polystyrene particles (green circle) of (a) volume of colloidal dispersion of 7 nm silica particles and 300 nm polystyrene particles for an air humidity of 1.3 % at 20 °C, (b) evaporation rate of 7 nm silica dispersion and 300 nm polystyrene dispersion with a volume of colloidal dispersion of 8 mm^3 at 20 °C, (c) silica particle size for an air humidity of 1.3 % at 20 °C and a volume of colloidal dispersion of 8 mm^3 and (d) polystyrene particle size for an air humidity of 1.3 % at 20 °C and a volume of colloidal dispersion of 8 mm^3.

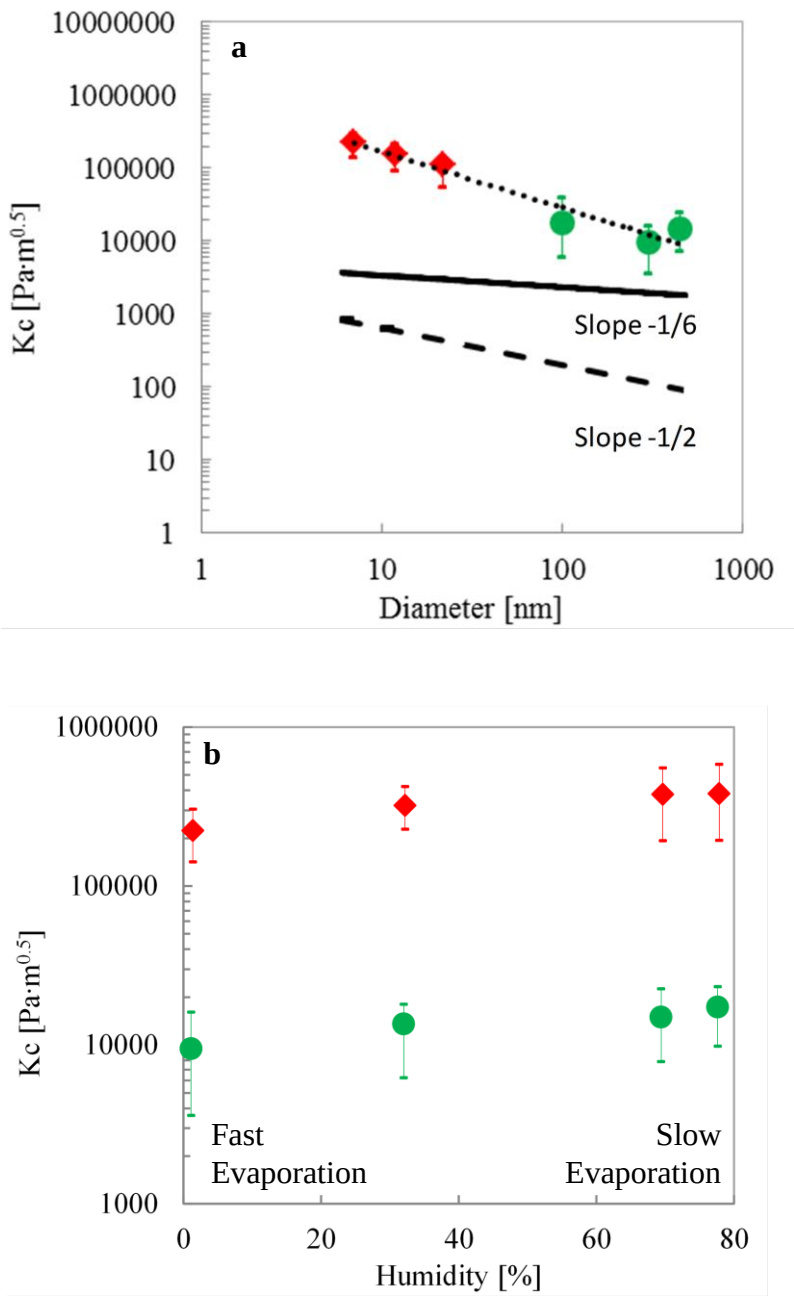

Figure 5: (a) Measured influence of particle size on fracture toughness of colloidal dispersions containing silica particles (red diamond) and polystyrene particles (green circle) for an air humidity of 1.3 % at 20 °C and a volume of colloidal dispersion of 8 mm^3. The best fir line has a slope of -0.8. (b) Measured influence of evaporation rate on fracture toughness of 7 nm colloidal silica (red diamond) and 300 nm polystyrene (green circle) for a volume of colloidal dispersion of 8 mm^3 at 20 °C.